JOURNAL OF MATERIALS SCIENCE 22 (1987) 592–600

Analysis of the strength and fracture behaviour of unidirectional and angle-ply graphite–aluminium composites

V. C. NARDONE, J. R. STRIFE
United Technologies Research Center, Silver Lane, East Hartford, Connecticut 06108, USA

The tensile behaviour of unidirectional and $[\pm\theta]_s$ angle-ply P100 graphite-reinforced 6061-Al composites was determined as a function of the angle (θ) between the fibre and the applied load. The experimentally determined values of the elastic modulus and tensile strength of the composites are compared with those predicted from classical laminate theory. The measured elastic modulus values agreed with theoretical values, but the strength of the $[\pm\theta]_s$ angle-ply composites was substantially greater than predicted. The discrepancy between experiment and theory is attributed to the stress required to fail the fibre ply/separator foil interface present in the angle-ply composites. The composite failure modes are also documented, and it is shown that the separator foils of the angle-ply composites shift the transition from tensile to shear failure to greater values of θ relative to the off-axis unidirectional composites.

1. Introduction

A unidirectional composite containing aligned fibres and stressed in tension at an angle to the fibre direction generally exhibits one of three distinct failure modes [1–5]. These are tensile failure of the fibre, shear failure of the fibre/matrix interface or the matrix itself, and tensile failure of the fibre/matrix interface or the matrix itself. The applied stress (σ_{APP}) necessary to cause failure by tensile fibre breakage is

$$\sigma_{APP} = \sigma_0/\cos^2\theta \quad (1)$$

where σ_0 is the failure stress for the composite parallel to the applied load and θ is the angle between the fibre axis and the applied load. The stress necessary to cause failure by this mode increases rapidly with increases in θ. Thus, tensile failure of the fibres is expected to dominate only for small values of θ.

Another type of failure that can occur is shear failure parallel to the fibre direction. Failure by shear occurs when

$$\sigma_{APP} = \tau/\sin\theta\cos\theta \quad (2)$$

The appropriate value for τ will be the lesser of the shear strength of the matrix material or shear strength of the fibre/matrix interface. This fracture mode generally dominates for a wide range of the intermediate values for θ.

The third mode of failure, which involves a tensile failure of the fibre/matrix interface or matrix itself, occurs when

$$\sigma_{APP} = \sigma_{90}/\sin^2\theta \quad (3)$$

where σ_{90} is the tensile strength of the composite when the fibres are oriented 90° to the applied stress. The tensile failure of the fibre/matrix interface or matrix generally dominates for large values of θ.

Equations 1 to 3 may be used to predict unidirectional composite strength in two different manners. The maximum stress theory predicts that the strength of the composite will be the least of the values for σ_{APP} in Equations 1 to 3. Alternatively, Equations 1 to 3 may be incorporated into Hill's maximum work theory [6] for yielding of an anisotropic material. When this is done, the composite is predicted to fail [7, 8] when

$$\frac{1}{\sigma_{APP}^2} = \frac{\cos^4\theta}{\sigma_0^2} + \left(\frac{1}{\tau^2} - \frac{1}{\sigma_0^2}\right)\cos^2\theta\sin^2\theta + \frac{\sin^4\theta}{\sigma_{90}^2} \quad (4)$$

Both the maximum stress and maximum work theories have been used to successfully predict unidirectional composite strength.

For the case of angle-ply composites, the maximum work theory predicts failure when

$$\frac{\sigma_x^2 - \sigma_x\sigma_y}{\sigma_0^2} + \frac{\sigma_y^2}{\sigma_{90}^2} + \frac{\sigma_s^2}{\tau^2} = 1 \quad (5)$$

where σ_x is the stress acting parallel to the fibres, σ_y is the stress acting perpendicular to the fibres and σ_s is the shear stress. Note that Equation 5 is simply a more general form for Equation 4. The values for σ_x, σ_y and σ_s can be calculated from laminate theory [9].

In this paper the strength and fracture characteristics of unidirectional and angle-plied composites are compared as a function of angle of the fibres with the applied stress. Fracture behaviour is examined in detail in order to account for the strength differences between the unidirectional and angle-ply composites tested relative to that predicted by the above failure criteria.

2. Materials and experimental procedure

2.1. Unidirectional composites

The unidirectional composite was fabricated by DWA

0022–2461/87 $03.00 + .12

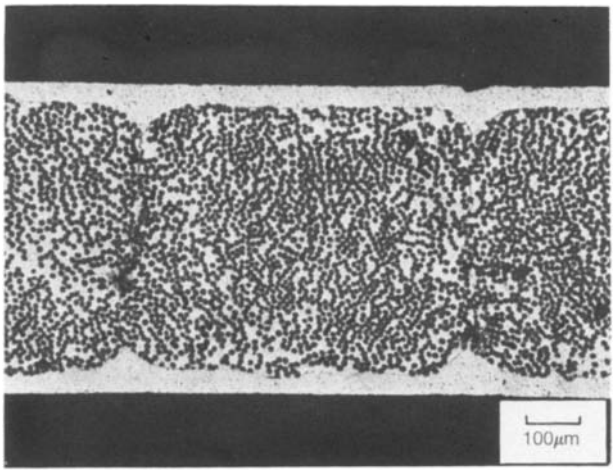

Figure 1 Microstructure of unidirectional P100/6061/6061-Al composite (V_f = 42.2%).

Composite Specialities, Inc. (Chatsworth, California), by diffusion-bonding a monolayer of P100/6061-Al precursor wire between 46 μm (1.8 mil) 6061 aluminium foil cladding. The P100/6061-Al wire was supplied by Materials Concepts, Inc. (Columbus, Ohio). The microstructure of the unidirectional composite is shown in Fig. 1. Fibre volume fraction in the fabricated composite was determined by acid dissolution as 42.2%. Tensile specimens were cut from the panels with a diamond saw at 0, 7.5, 15, 30 and 90° to the fibre direction. Fibreglass doublers were adhesive-bonded to the tensile specimens providing a gauge length from 2.54 to 5.08 cm. (For the 0° specimens, steel doublers were used). The specimen width was 0.76 cm in all cases. All tensile specimens had resistance strain gauges mounted to both sides and were loaded at a constant crosshead deflection rate of 0.0254 cm min^{-1}. The composite was tested in the as-fabricated condition.

2.2. Angle-ply composites

Four-ply panels with fibre orientations of $[\pm 11]_s$, $[\pm 14]_s$, $[\pm 20]_s$, $[\pm 23]_s$, and $[\pm 26]_s$ were consolidated by DWA Composite Specialties, Inc. using vacuum diffusion bonding of plies constructed from collimated P100/6061-Al liquid-metal infiltrated wires. The wires were supplied by Materials Concepts, Inc. Foils of 6061 aluminium were used between the fibre plies and as cladding for the composite. The 6061-Al separator foils were 46 μm in thickness for all composites, while the cladding thickness varied among the composites as reported in Table I. A typical microstructure for an angle-ply composite is shown in Fig. 2. A summary of the fibre volume fraction of each panel is also listed in Table I as determined from acid dissolution. Tensile specimens were cut from the panels with a diamond saw in the longitudinal direction. Transverse specimens were also cut from the $[\pm 11]_s$, $[\pm 20]_s$ and $[\pm 26]_s$ composites and are reported as $[\pm 79]_s$, $[\pm 70]_s$ and $[\pm 64]_s$ angle-ply composites, respectively. Fibreglass doublers were adhesive-bonded to the tensile specimens providing a gauge length from 3.81 to 8.89 cm. The specimen width was either 0.76 or 1.52 cm. The tensile testing procedure was identical to that used in the testing of the unidirectional composites. The composites were tested in the as-fabricated condition except for two longitudinal $[\pm 23]_s$ specimens and three longitudinal $[\pm 20]_s$ specimens where the matrix was heat-treated to a T6 condition.

TABLE I Volume fraction of P100 fibres and cladding thickness of the angle-plied composites

Panel	Angle	Volume fraction (%)	Cladding thickness (μm)
4951	±11	43.6	90
5274	±14	37.7	90
5685	±20	41.7	90
5369	±23	42.3	90
4870	±26	44.7	25

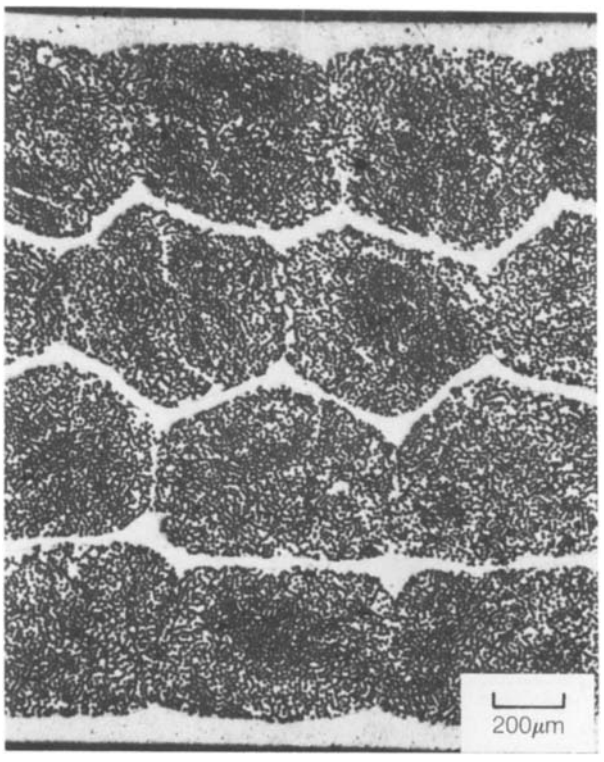

Figure 2 $[\pm 11]_s$ P100/6061/6061-Al microstructure.

3. Experimental results

3.1. Unidirectional composites

The mechanical properties of the unidirectional composite are summarized in Table II. Initially, there is a sharp drop in strength and modulus as the angle (θ) between the tensile axis and fibre orientation increases. The loss of strength and modulus tends to saturate as the value for θ becomes greater than 30°. Typical stress–strain curves with the stress axis aligned at θ = 0, 15 and 90° to the fibre direction are shown in Fig. 3.

Optical micrographs of gauge section failures for all five test orientations are shown in Fig. 4. Only the 0° samples showed fibre breakage across the width of the specimen, although the 7.5° sample displayed some fibre breakage near the central portion of the sheared fracture surface. For the other θ values, the fracture surfaces are macroscopically smooth and failure occurs parallel to the fibre direction. The 15 and 30°

TABLE II Tensile properties of the single-ply unidirectional composite

Fibre orientation with tensile axis (deg)	E (GPa)	UTS (MPa)	ε_f (%)*
0	332	753	0.236
	334	736	0.233
Average value	333	745	0.2345
7.5	267	214	–
15	162	126	0.113
	157	124	0.145
Average value	160	125	0.129
30	61.5	49.5	0.174
	61.7	47.3	0.098
	–	56.5	–
Average value	61.6	51.1	0.136
90	–	17.0	–
	27.5	21.9	0.113
	30.3	–	–
	29.2	22.9	0.094
	28.1	21.9	0.091
	29.8	–	–
Average value	29.0	20.9	0.099

*Strain to failure.

samples display a pure shear failure, while the 90° sample exhibits a transverse tensile failure.

Higher magnification SEM micrographs of the 0, 15 and 90° fracture surfaces are presented in Figs 5 to 7. The 0° fracture surface shows extensive pullout and tensile fibre failure. The 15 and 90° fracture surfaces are similar from the standpoint that the fibres generally lay parallel to the fracture surface and there is substantial evidence of fibre/matrix decohesion. The fracture surfaces appear to differ, however, in that the 15° shear surface exhibits substantial evidence of matrix peeling and coiling in the shear direction. A higher magnification view of the matrix coiling is given in Fig. 8. The arrow indicates the direction of the shear stress acting on the shear fracture surface (see discussion below).

3.2. Angle-ply composites

The mechanical properties of the angle-ply composites are summarized in Table III. While the data exhibit a loss of strength with an increase in fibre angle to the stress axis (θ), this loss is significantly less than that observed for unidirectional composites tested at comparable angles of θ when θ is less than 30°. The $[\pm 64]_s$, $[\pm 70]_s$ and $[\pm 79]_s$ angle-ply composites exhibited equivalent strength to the 90° unidirectional samples. Typical stress–strain curves for the angle-ply composites are presented in Fig. 9. Given in Table IV are the effects of heat treatment and specimen width on the strength of the $[\pm 20]_s$ and $[\pm 23]_s$ composites.

An optical micrograph of the gauge section failures for the $[\pm 11]_s$, $[\pm 14]_s$, $[\pm 20]_s$, $[\pm 23]_s$ and $[\pm 26]_s$ composites is shown in Fig. 10. A pure shear failure is only evident in the $[\pm 23]_s$ composite. For smaller fibre orientations with the stress axis, shear initiates on a given fracture plane but is interrupted by fibre failure in the mid-section of the specimen. The failure changes back to shear failure once again on the opposite side of the specimen. This is clearly evident in the $[\pm 11]_s$ and $[\pm 14]_s$ composites. Note that the proportion of tensile fibre failure to shear failure decreases as θ increases. A higher magnification of the $[\pm 23]_s$ failure surface is presented in Fig. 11. A pure shear failure mode is observed and the separator foil is observed on the fracture surface.

An optical micrograph of the gauge section failures of the $[\pm 64]_s$, $[\pm 70]_s$ and $[\pm 79]_s$ composites is shown in Fig. 12. The outer fibre plies exhibited a shear-type failure parallel to the fibre orientation, but the inner plies showed extensive fibre breakage. A view of the

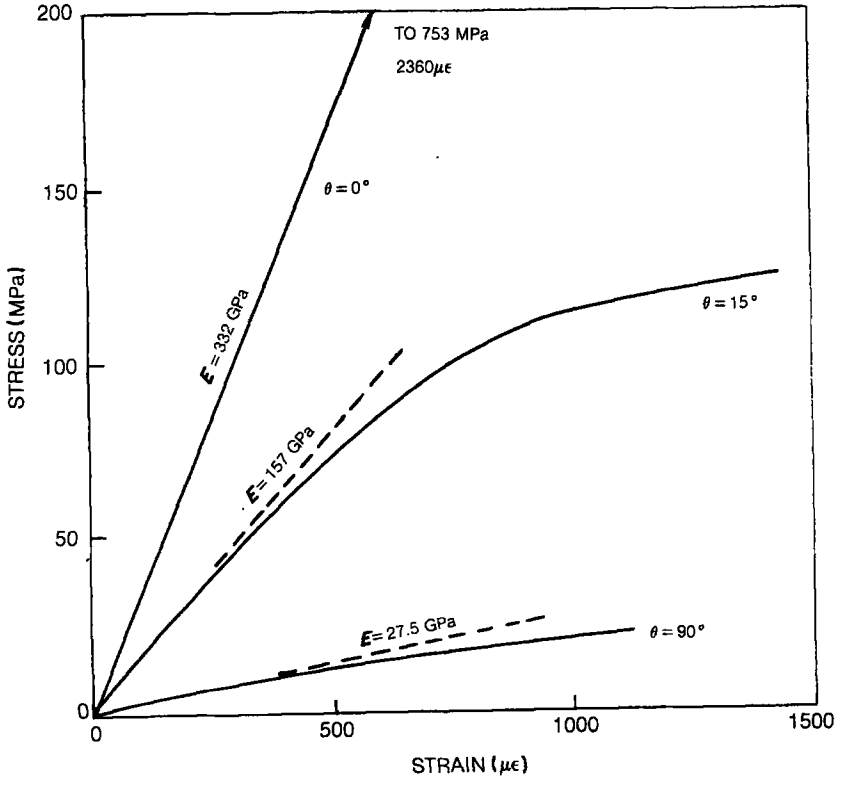

Figure 3 Tensile behaviour of unidirectional P100/6061/6061-Al as a function of fibre angle, θ, with the tensile axis. V_f = 42.2%.

TABLE III Tensile properties of the four-ply $[\pm\theta]_s$ angle-ply composites

Panel	Orientation of fibre with tensile axis	E (GPa)	UTS (MPa)	ε_f (%)
4951	±11	305	473	0.181
		300	495	0.201
		309	502	0.203
	Average value	305	490	0.195
5274	±14	244	428	0.287
		233	420	0.266
		256	373	0.229
	Average value	244	407	0.261
5685	±20	243	302	0.234
		248	299	0.176
		242	313	0.198
	Average value	245	305	0.203
5369	±23	190	223	0.296
		197	211	0.198
		191	222	0.165
	Average value	193	219	0.220
4870	±26	129	155	0.260
		125	163	0.275
		126	166	0.315
		142	161	0.255
	Average value	131	161	0.276
4870	±64	20.6	24.4	0.196
		17.8	27.3	0.295
		20.2	24.8	0.199
	Average value	19.5	25.5	0.230
5685	±70	30.4	28.5	0.257
		28.8	26.9	0.192
		31.4	28.0	0.261
	Average value	30.2	27.8	0.237
4951	±79	26.6	26.7	0.188
		27.2	26.9	0.248
	Average value	26.9	26.8	0.218

fracture plane for the $[\pm 70]_s$ composite is presented in Fig. 13.

4. Discussion

4.1. Modulus and strength of the composite materials

A comparison of the predicted and experimentally determined average elastic modulus values for both the unidirectional and angle-ply composites is given in Fig. 14. The calculated values were obtained using laminate theory [9] and the experimentally determined values for the unidirectional longitudinal elastic modulus (333 GPa), transverse elastic modulus (29 GPa) and Poisson's ratio (0.27). The shear modulus value (17 MPa) was estimated by fitting the data to the observed value for the 7.5° orientation of the unidirectional composite.

The correlation of the predicted and actual values is fairly good, particularly for the unidirectional composite. For the angle-ply composite, the experimentally determined elastic modulus values from panels 5274 and 4870 are somewhat less than predicted. The low value for the $[\pm 14]_s$ orientation may be attributed to the low fibre volume fraction in the composite relative to the others (see Table I). For the $[\pm 26]_s$ orientation, it should be noted that the cladding thickness is relatively small. This could result in lower shear

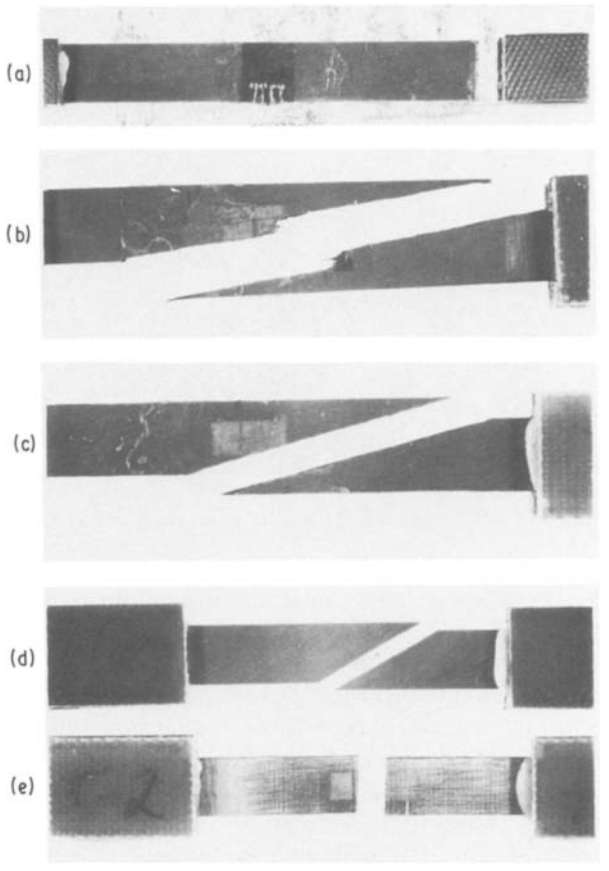

Figure 4 Failure modes exhibited by unidirectional composites as a function of fibre orienation. (a) 0°, (b) 7.5°, (c) 15°, (d) 30°, (e) 90°.

and transverse modulus values and therefore a more rapid decrease in modulus with increasing θ value would be anticipated.

Two means of predicting composite strength are by the maximum stress and maximum work failure criteria. The maximum stress criterion predicts that failure occurs when the resolved stress due to the applied load is sufficient to cause longitudinal fibre

TABLE IV Effect of heat treatment and specimen width on composite strength

Specimen*	Width (cm)	UTS (MPa)	E (GPa)
$[\pm 23]_s$–F	0.76	223	190
		211	197
		222	191
	Average value	219	193
$[\pm 23]_s$–T6	0.76	238	161
$[\pm 23]_s$–T6	1.52	325	153
$[\pm 20]_s$–F	0.76	302	243
		299	248
		313	242
	Average value	305	245
$[\pm 20]_s$–T6	0.76	339	228
		340	228
		342	229
	Average value	340	228
$[\pm 20]_s$–F	1.52	421	246
		418	251
	Average value	420	248

*F = as-fabricated; T6 = 530° C for 1 h/water quench; 163° C for 18 h.

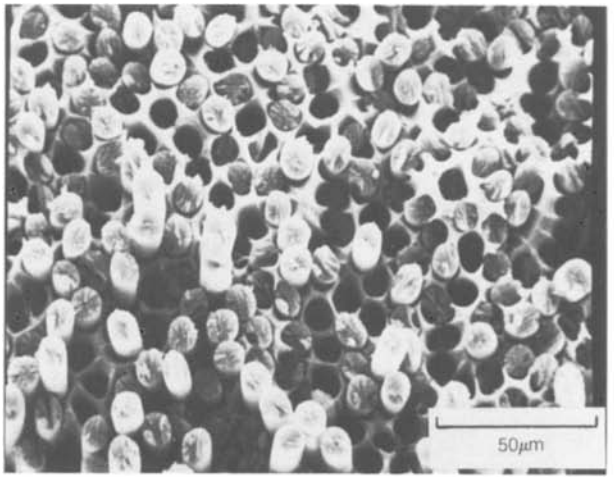

Figure 5 Fracture surface of the unidirectional composite at $\theta = 0°$.

Figure 7 Fracture surface of the unidirectional composite at $\theta = 15°$.

breakage, shear failure or transverse failure. Thus, if this criterion were to apply, one would anticipate distinct regions where each of the respective failure modes would occur. Further, the strength of the composite is predicted to be a discontinuous function of θ. In contrast, the experimental results exhibit a continuous decrease in strength (see Fig. 15) and a gradual change (see below) from primarily fibre failure to shear failure with increasing values of θ. Since these experimental results are not consistent with the assumptions made in the maximum stress failure criterion, only the maximum work failure criterion will be used to calculate composite strength.

A comparison of the actual and predicted strength values for both the unidirectional and angle-ply composites is given in Fig. 15. The unidirectional composite strength was predicted using Equation 4 with the experimentally determined values of σ_0 (750 MPa), and σ_{90} (21 MPa). The value for the shear strength, τ, was estimated from a best fit with the unidirectional composite data as 31 MPa. The correlation between the calculated and actual strength values is very good.

A comparison of the predicted (Equation 5) and actual average strength values for the angle-ply composites is also given in Fig. 15. In this case, the calculated values for $\theta < 26°$ are consistently less than the experimentally determined strength values when the unidirectional values for σ_0, σ_{90} and τ are used. The magnitude of τ necessary to account for the strength of the angle-ply data is much larger than the value for τ used to predict unidirectional composite strength. These results indicate that the shear process is more difficult for the angle-ply composite relative to the off-axis unidirectional composites, when the value for θ is small.

It is postulated that the difference in the shear behaviour between the unidirectional and angle-ply composites is due to the presence of the matrix foils that separate the fibre plies, which introduce an additional barrier to the shear process. As is the case for the unidirectional material, shear failure of a given ply in the angle-ply composite occurs by failure of the fibre/matrix interface parallel to the fibre direction. However, the shearing ply in an angle-ply composite must also overcome the bond of the fibre ply to the separator foil over the entire area of foil between it and an adjacent ply. The added stress necessary to cause failure of the fibre ply/separator foil interface can explain why the shear process is more difficult in the angle-ply composites relative to the unidirectional composites.

The exposed surface of the separator foil is evident in the micrograph of the $[\pm 23]_s$ composite as shown in Fig. 11. Notice that the fibre bundle imprints in the separator foil are oriented in the same direction as those in the outer ply that was once above it. This is experimental confirmation that failure of the fibre ply/separator foil interface occurs during the shear process in an angle-ply composite. This feature was charateristic of all the lower θ ($< 26°$) angle-ply composites.

It should also be noted that the area of the fibre ply/separator foil interface that fails during the shearing of an angle-ply composite decreases as θ increases. Therefore, the strengthening contribution due to this mechanism will be large for small values of θ, and continuously decrease as the value of θ increases. This explains why the strength of the higher θ ($> 60°$) angle-ply composites is not underestimated by the maximum work failure criterion (see Fig. 15), even though the unidirectional value for τ was used.

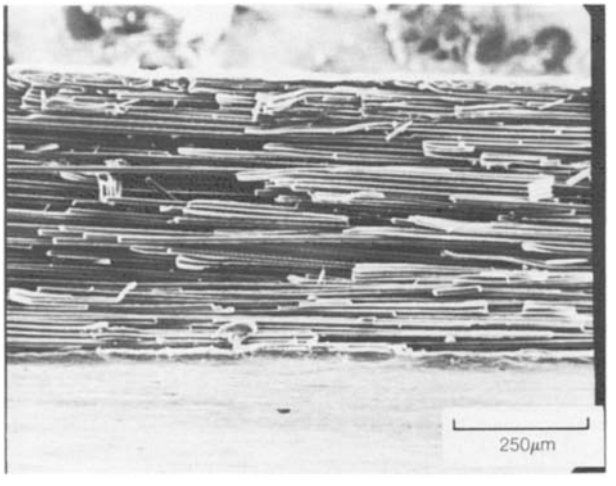

Figure 6 Fracture surface of the unidirectional composite at $\theta = 90°$.

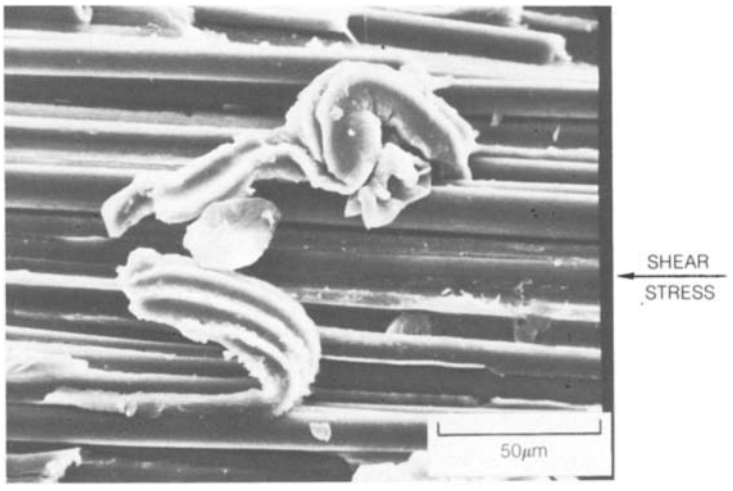

Figure 8 Fracture surface of the unidirectional composite at $\theta = 15°$, highlighting matrix coiling.

If failure of the fibre ply/separator foil interface does indeed contribute substantially to angle-ply composite strength, a very important point may be inferred. The areas of fibre ply/separator foil interface that must fail in order for the angle-ply composite to shear is equal to $1/2\, w^2 \cot \theta$, where w is the specimen width. Therefore, the force necessary to fail the interface will be proportional to $\tau'\, w^2 \cot \theta$, where τ' is the strength of the fibre ply/separator foil interface. In contrast, the force acting on the composite will be proportional to $\sigma_{APP}\, wt$, where t is the specimen thickness. Equating these two expressions for the force gives

$$\sigma_{APP} \propto \frac{\tau' w \cot \theta}{t} \tag{6}$$

Equation 6 suggests that the σ_{APP} necessary to fail the fibre ply/separator foil interface will increase as the specimen width increases and θ decreases.

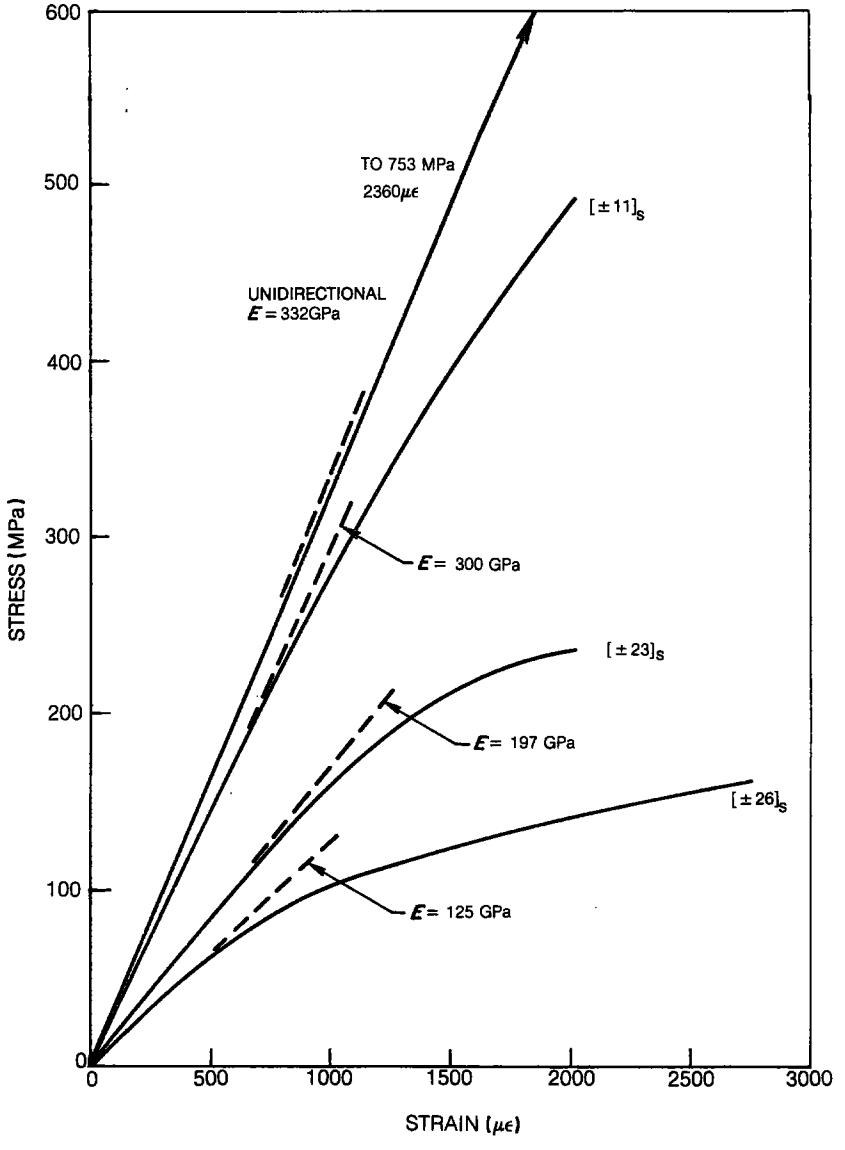

Figure 9 Longitudinal tensile behaviour of P100/6061/6061-Al composites.

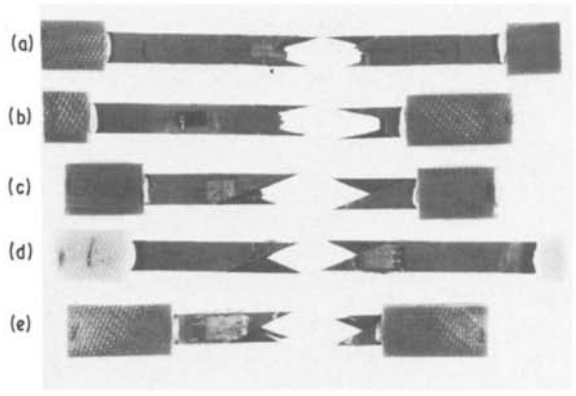

Figure 10 Failure modes of the angle-ply composites as a function of fibre orientation. (a) $[\pm 11]_s$, (b) $[\pm 14]_s$, (c) $[\pm 20]_s$, (d) $[\pm 23]_s$, (e) $[\pm 26]_s$.

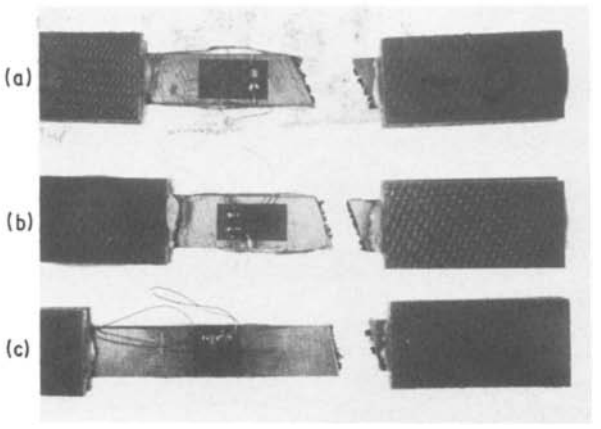

Figure 12 Failure modes of the angle-ply composites with large values of $[\pm\theta]_s$. (a) $[\pm 64]_s$, (b) $[\pm 70]_s$, (c) $[\pm 79]_s$.

The effect of specimen width on the strength of two angle-ply composites is shown in Table IV and Fig. 15. Note that when the specimen width is doubled, the ultimate tensile strength of the composite is increased by about 30 to 40%. These experimental results argue strongly in favour of the hypothesis that failure of the fibre ply/separator foil interface contributes significantly to the composite shear strength, which in turn substantially increases the ultimate tensile strength of the angle-ply composites for smaller values of θ ($< 30°$). Also shown in Table IV is the effect of heat treatment on composite strength. Note that only modest increases in strength occur, which suggest that failure of the separator foils themselves contributes only slightly to the observed angle-ply composite strength. This result is anticipated, since a T6 heat treatment should increase the tensile strength of the 6061-Al matrix foils from 124 to 310 MPa, and these foils occupy about 15% of the composite by volume. The estimated increase in strength due to a T6 heat treatment is thus 28 MPa, which compares favourably with the observed increase of 35 MPa for the $[\pm 20]_s$ composite.

4.2. Fracture surface analysis

The failure of the unidirectional composite oriented 0° to the applied load shows extensive fibre pullout and breakage (see Fig. 5). This is representative of the typical failure mode that is apparent for 0° composite specimens.

The fracture surface of the 15 and 30° unidirectional specimens (Fig. 4) represents a pure shear failure that is continuous across a single plane. For the 7.5° specimen, the fracture surface displays a step near the midplane of the specimen where fibre breakout is evident. These results imply that as the length of the shear surface becomes large, i.e. as θ decreases and the stress to cause shear failure increases, there is a tendency for a mixed failure mode to occur. This suggests that there is no abrupt change from shear to fibre tensile failure at some critical θ value, but rather a transition region where the fracture surface displays both shear and tensile regions of failure. The lower the value for θ, the greater the ratio of the tensile to shear failure regions.

The fracture surfaces of the specimens failing in shear and transverse tension show fibre surfaces with no adherent matrix as well as sheaths of matrix

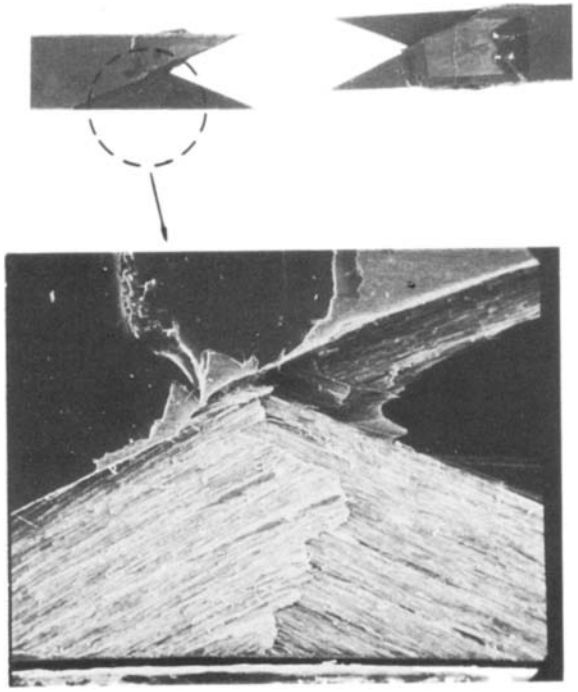

Figure 11 Shear failure mode of the $[\pm 23]_s$ angle-ply composite.

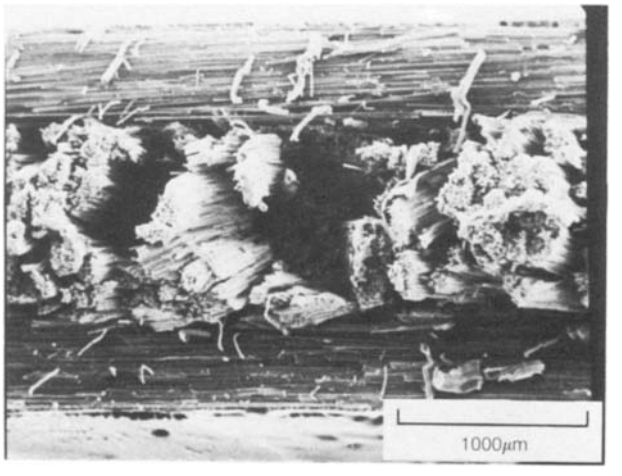

Figure 13 Fracture surface of the $[\pm 70]_s$ angle-ply composite.

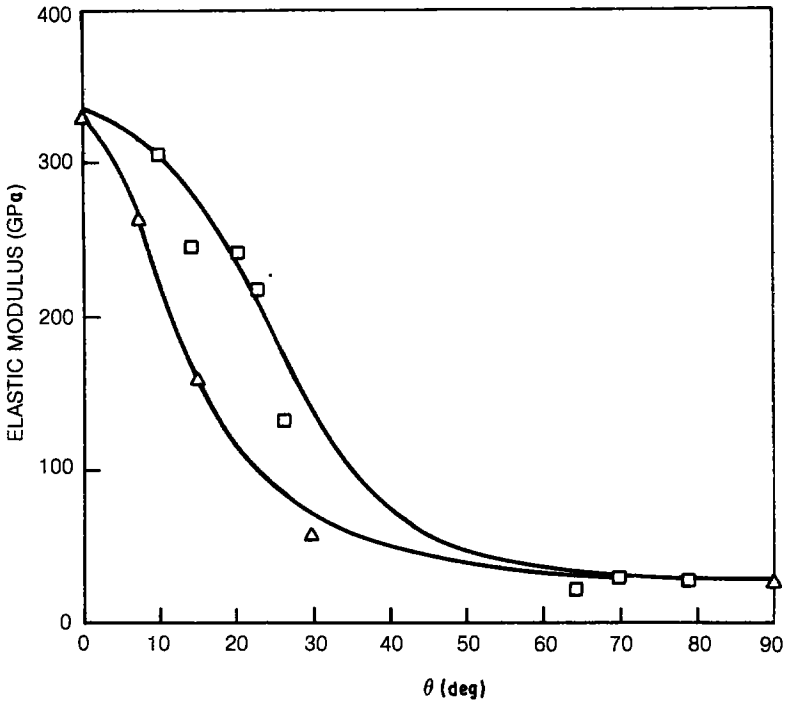

Figure 14 Modulus as a function of θ for both the unidirectional and angle-ply composites. Average values from Tables II and III: (△) unidirectional, (□) angle-ply.

material where a fibre once laid (see Figs 6 and 7). The results indicate that failure is controlled by decohesion of the fibre/matrix interface in both cases as opposed to matrix failure.

A difference between the transverse and shear failure modes is the presence of somewhat more matrix coiling on the shear fracture surface. As the fibre/matrix interface fails during the shear process, portions of the separated matrix are coiled into clumps. These matrix coils are invariably found adjacent to areas of the matrix that remained adherent to the fibre, and are coiled in the same direction as the shear stress acting at the fracture surface. An SEM micrograph that is characteristic of the matix coiling at a shear fracture surface is shown in Fig. 8. Thus, a possible way to distinguish between a shear and transverse fracture surface has been established.

In contrast to the predominance of shear failure for the unidirectional composites, only one of the eight $[\pm\theta]_s$ angle-ply composites tested exhibits a pure shear failure. A pure shear failure is evident for the $[\pm 23]_s$ composites, but different failure modes are evident for both higher and lower values of θ. The $[\pm 11]_s$ and $[\pm 14]_s$ specimens exhibited fracture behaviour that is similar to that evident for the 7.5° unidirectional specimen. Specifically, failure by shear begins to initiate on a given plane, then there is fibre failure near the midplane of the specimen, followed by a shear-type failure on another fracture plane. The region of fibre failure near the midplane of the specimen is much larger in magnitude for the angle-ply composites relative to the unidirectional sample.

It was postulated that the fibre breakage occurs when the shear distance in the unidirectional composite

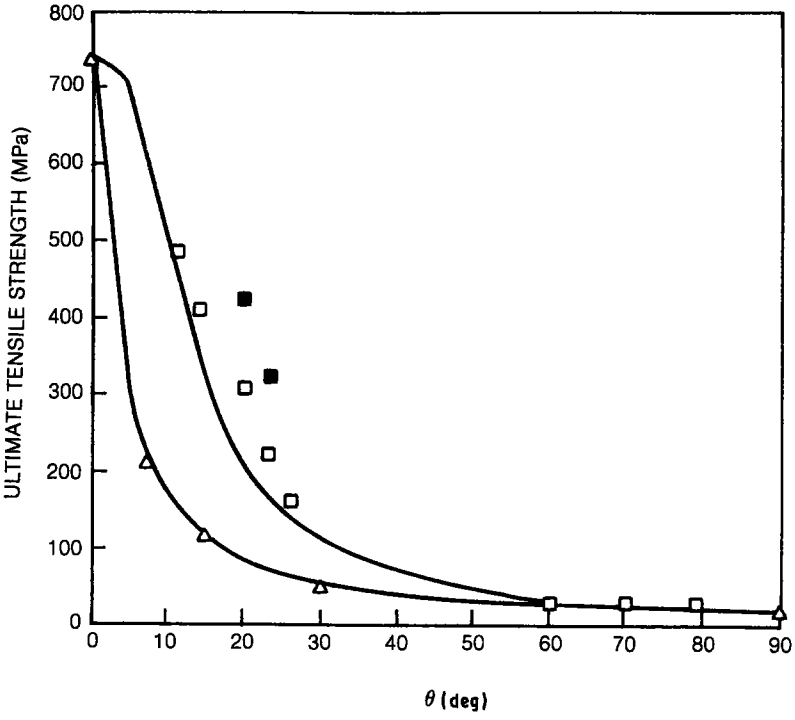

Figure 15 Strength as a function of θ for both the unidirectional and angle-ply composites. Average values from Tables II, III and IV: (△) unidirectional, (□) 0.76 cm wide angle-ply; (■) 1.52 cm wide angle-ply specimens.

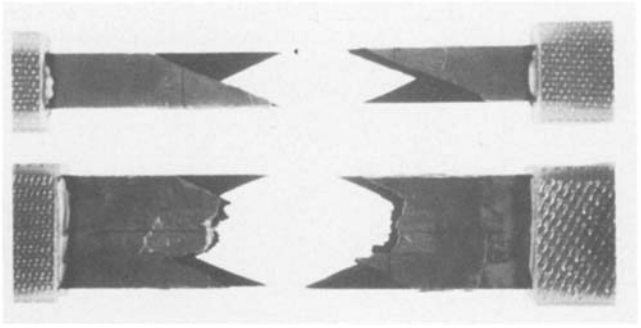

Figure 16 Failure modes of $[\pm 23]_s$ composites showing transition to mixed mode from pure shear as the specimen width increases.

becomes large, i.e. when the stress necessary to cause shear failure becomes large. The extensive fibre breakage evident in the $[\pm 11]_s$ and $[\pm 14]_s$ angle-plied composites suggest that the shear process is more difficult relative to the unidirectional material tested off-axis at the same angle, and therefore more extensive tensile fibre failure is favoured. Note that the unidirectional specimens tested at 15° off-axis showed pure shear failure. In the prior discussion on the strength of the angle-ply composites, it was pointed out that in order for shear to occur, failure of the fibre/matrix interface must be accompanied by failure of the fibre ply/separator foil interface. The added stress necessary to overcome the resistance of the fibre ply/separator foil interface makes shear more difficult in the angle-plied composites relative to the unidirectional composites tested at a given value of θ. Thus, the fibre breakage failure mode near the midplane of the specimen is more extensive for any given value of θ.

The prior discussion concerning width-dependent specimen strength suggests that more extensive fibre breakage should also occur for a given θ value as the specimen width increases, since the shear process is more difficult. Tensile failures for $[\pm 23]_s$ specimens are compared at different widths in Fig. 16. Note that the wider specimen shows a mixed failure mode, while the thinner specimen fails in pure shear. The $[\pm 20]_s$ specimens also showed a greater fraction of tensile fibre failure as the width increased. The greater proportion of tensile fibre failure in specimens of greater width is further support of the hypothesis that the shearing process becomes more difficult as specimen width increases.

Different failure modes are observed for the angle-ply composites at greater ply angles. The $[\pm 26]_s$ composite superficially appears to fail by shear, but there is evidence of separation within the plies. The failure mode of angle-ply composites where $\theta > 60°$ is characterized by shear failure on the outer two plies but extensive fibre breakage on the inner plies (See Fig. 13). When a given ply begins to shear, it imposes a stress on a differently oriented ply that is transmitted by the separator foil. Instead of failure of the fibre ply/separator foil interface, failure can be induced on the non-shearing ply. The net result is failure by fibre breakage in the non-shearing plies provided that the ply angle is sufficiently large, or failure of the fibre/matrix interface due to ply rotation. This effect is currently being studied in quasi-isotropic $[0 \pm 60]_s$ laminates.

5. Conclusions

1. The strengths of angle-ply composites are greater than unidirectional composites tested at similar angles of fibre orientation, θ, with the stress axis for fibre orientations $\theta < 30°$.

2. Although higher strength values are analytically predictable for the angle-plied composites, the experimentally observed increases were significantly greater than calculated from the maximum work failure criteria.

3. The additional strength increment observed for the angle-ply composites over the predicted values is due to the increased stress required to fail the fibre ply/separator foil interface in these composites.

4. Both the unidirectional and angle-plied composite fracture surfaces possess shear and tensile fibre failure regions when the value for θ is small. The fraction of tensile fibre failure increases as θ decreases, since the shear process becomes more difficult as θ decreases. The angle-ply specimens exhibit a greater fraction of tensile fibre failure for any given value of θ, since the shearing process is more difficult.

5. The failure mode of angle-ply composites with $\theta > 60°$ is characterized by shear failure of the outer two plies but extensive fibre breakage of the inner plies. Unidirectional composites exhibit fibre–matrix decohesion in this test regime.

6. The strength of angle-ply composites is a function of the test specimen width for composites incorporating ply separator foils. Also, the fraction of fibre tensile failure relative to shear failure increases as the specimen width increases for a given value of θ.

Acknowledgement

The support of the Air Force Wright Aeronautical Laboratories under Contract F33615-81-C-5128 in performing this research is gratefully acknowledged.

References

1. E. Z. STOWELL and T. S. LIU, *J. Mech. Phys. Solids* **9** (1961) 242.
2. A. KELLY and J. G. DAVIES, *Met. Rev.* **10** (1965) 1.
3. P. W. JACKSON and D. CRATCHLEY, *J. Mech. Phys. Solids* **14** (1966) 49.
4. G. A. COOPER, *ibid.* **14** (1966) 103.
5. A. KELLY, "Strong Solids" (Clarendon Press, Oxford, 1966) p. 150.
6. R. HILL, "The Mathematical Theory of Plasticity" (Clarendon Press, Oxford, 1950) p. 317.
7. S. W. TSAI, in "Fundamental Aspects of Fibre Reinforced Platic Composites", Vol. 3, edited by R. T. Schwartz and H. S. Schwartz (Interscience, New York, 1968) p. 3.
8. *Idem*, "Strength Characteristics of Composite Materials", NASA CR-224 (NASA, Washington, 1965).
9. J. C. HALPIN, "Primer on Composite Materials: Analysis" (Technomic Publishing Co., Lancaster, Pennsylvania, 1984) p. 35.

Received 3 April
and accepted 5 June 1986